Combining mesenchymal stem cells with a nutritional intervention of lysophosphatidylcholine docosahexaenoic acid: the future treatment for perinatal hypoxia-ischemia?

Abstract

Background Perinatal hypoxia-ischemia (HI) is the leading cause of morbidity and mortality among infants worldwide. Currently, the only approved treatment for infants suffering from HI injury is hypothermia, which has a lot of limitations. Hence, there is a pressing need for new therapies. One promising option in the treatment of perinatal HI is mesenchymal stem cell (MSC) therapy, which is effective in reducing lesion size and improving motor and cognitive impairment. However, there is still room to optimise this MSC therapy. Nutritional interventions might be a viable new option, as they can be rapidly implemented in the clinic and are generally considered safe. One such nutritional intervention is the omega-3 fatty acid docosahexaenoic acid (DHA), which has neuroprotective effects by acting anti-apoptotic, anti-inflammatory, and pro-regenerative. DHA bound to lysophosphatidylcholine (LPC) seems to lead to targeted enrichment of brain DHA and corresponding functional improvement. Therefore, this study combined LPC-DHA with MSC therapy to increase the treatment effect in a mouse model of perinatal HI. Besides, *in vitro* neuronal cell culture experiments were performed to unravel the mechanisms behind (LPC-)DHA treatment.

Methods C57Bl/6 mice were subjected to HI injury at postnatal day 9 (P9) followed by a daily oral gavage of LPC-DHA between P9 and P15. At P12, MSCs were administered intranasally to the HI injured mice. At P37, brains were collected and used for immunohistological analysis. Coronal sections at bregma level -1.34 were stained for microtubule-associated protein 2 (MAP2), myelin basic protein (MBP), and chicken ovalbumin upstream promoter transcription factor-interacting protein 2 (CTIP2) to examine the grey matter, white matter, and cortical organization, respectively. *In vitro,* the anti-inflammatory effects of DHA were examined in primary microglia cultures. Besides, the neuroprotective effects of both DHA and LPC-DHA were examined in H_2O_2, etoposide and oxygen glucose deprivation (OGD) hit models using the neuronal SH-SY5Y cell line.

Results A combined treatment of LPC-DHA with MSCs can decrease grey matter loss and restore the balance of deeper layer pyramidal neuron density within the somatosensory cortex of HI injured mice, whereas separate treatments with LPC-DHA or MSCs could not. Moreover, our *in vitro* studies show DHA has anti-inflammatory effects and increases cell viability after an H_2O_2 and OGD hit, but not after an etoposide hit. LPC-DHA also increases cell viability after an H_2O_2 hit, but decreases cell viability after an etoposide or OGD hit.

Conclusion Our study indicates a combined treatment with LPC-DHA and MSCs aids in brain recovery after perinatal HI in mice. The action of LPC-DHA is possibly exhibited by anti-oxidant, anti-inflammatory and proliferative action. Future research should further optimize and unravel the mechanism behind a treatment combining LPC-DHA and MSCs to take the next step towards improved treatment for infants suffering from perinatal HI.

Keywords: Perinatal hypoxia-ischemia; Mesenchymal stem cells; Lysophosphatidylcholine; Docosahexaenoic acid.

Plain language summary

A baby can get hurt during birth, because it cannot get enough oxygen and sugar. Later in life, problems can become clear, when the child can get difficulties with making movements and performance in school. These problems happen because brain cells have died due to the lack of oxygen and sugar. Imagine this state of the brain as a glass jar that has fallen and now contains cracks. Currently, the only treatment babies can get to repair these cracks, is cooling of the complete body. By cooling the body, further rupture of the cracks is prevented, but restoring the cracks is not possible. Therefore, a new therapy is urgently needed. A kind of super cells, called stem cells, are believed to provide the glue to restore these cracks. However, how good this glue works can be improved. It is known the brain has some ability to restore its own cracks if it gets enough tools. One tool that can be given is fat. Fat is known to support the self-healing process after damage. Therefore, the effect of combining the super cells with fat to restore the cracks in the brain is studied.

In our study, mice got brain damage 9 days after birth as this is comparable to a human baby at birth. Right after injury up until the mice were 15 days old, they received fat daily. On top of that, the mice received super cells at day 12. At adult age, it could be determined if the damage was restored by looking inside the brains. The brain cells were indeed repaired by our treatment. Besides, by looking at a specific part of the brain that is involved in movements and memory, it was found the organization in the brain was disrupted after the baby got hurt. Though, our combined treatment with the super cells with fat was able to restore the balance in brain organization.

In addition to the study in mice, brain cells in a dish were also studied to see more specifically which tools the fat offers to the brain. The brain cells were treated with two types of fat; a simple form of fat and a complex fat for the brain, which was used in the mice. These tests showed both types of fat make our brain cells healthier. Besides, the brain cells were injured to see which types of tools the fats possess. Firstly, the brain cells were injured by adding a lot of stress molecules. Both forms of fat had tools to protect the brain cells against stress. Next, the cells were damaged by cutting their DNA. In this case, both forms of fat did not have tools to protect the brain cells. Lastly, oxygen and sugar were temporarily taken away from the brain cells. Here, only the simple form, but not the complex fat possessed tools to protect the brain cells.

Taking our findings together, it is suggested the complex fat helps the super cells by repairing brain cells and protecting them against stress and injury.

1. Introduction

Perinatal HI is the leading cause of morbidity and mortality among infants worldwide (1). Approximately 3 in 1000 newborns suffer from perinatal HI, of which 24% dies at the neonatal intensive care unit (NICU) (2). HI injury has various consequences for the surviving infants, such as cerebral palsy, visual and auditory problems, and motor and behavioural difficulties later in life (3–5). These motor and behavioural difficulties vary from epilepsy, delayed mental development, autism, and even seizures (2).

Currently, the only approved treatment for perinatal HI is hypothermia (6). During hypothermia, the body is cooled to 33.5 °C for 72 hours to protect the brain against injury (7). Although hypothermia is safe, improves the chance of survival, and reduces cerebral palsy, this treatment has a short treatment window of 6 hours after the ischemic event, only gives partial protection, and is not effective when infants have moderate to severe brain damage (2,8–11). Considering these limitations, there is a high need for a better treatment option.

During perinatal HI, a temporary, but abrupt decrease in cerebral blood flow activates many processes in the brain (Fig 1). The brain will temporarily lack oxygen and glucose, which leads to a decreased adenosine triphosphate (ATP) production. Besides, the level of brain DHA, an omega-3 fatty acid essential for brain development, decreases after HI (12,13). After HI, the brain is reperfused and the low ATP levels lead to a compensating excess of calcium, causing excitotoxicity and oxidative stress. The oxidative stress and excitotoxicity cause an increase of reactive oxygen species (ROS) and necrosis by which damage associated molecular patterns (DAMPs) are released. DAMPs activate pro-inflammatory pathways leading to apoptosis. Another result from reperfusion is the further decrease of the DHA level in the brain as DHA is released to produce bioactive lipid mediators, like neuroprotectin D1 (NPD1) (14,15). NPD1 activates pro-survival and anti-apoptotic signalling pathways to limit damage (16). Moreover, from approximately 3 days after the initial injury astrogliosis, late cell death and repair and remodelling occurs (3). Despite these protective mechanisms of the brain, a significant lesion and DHA shortage in the brain endures (17,18). Accordingly, newborns suffering from perinatal HI need a proper therapy to protect and restore the brain after HI injury.

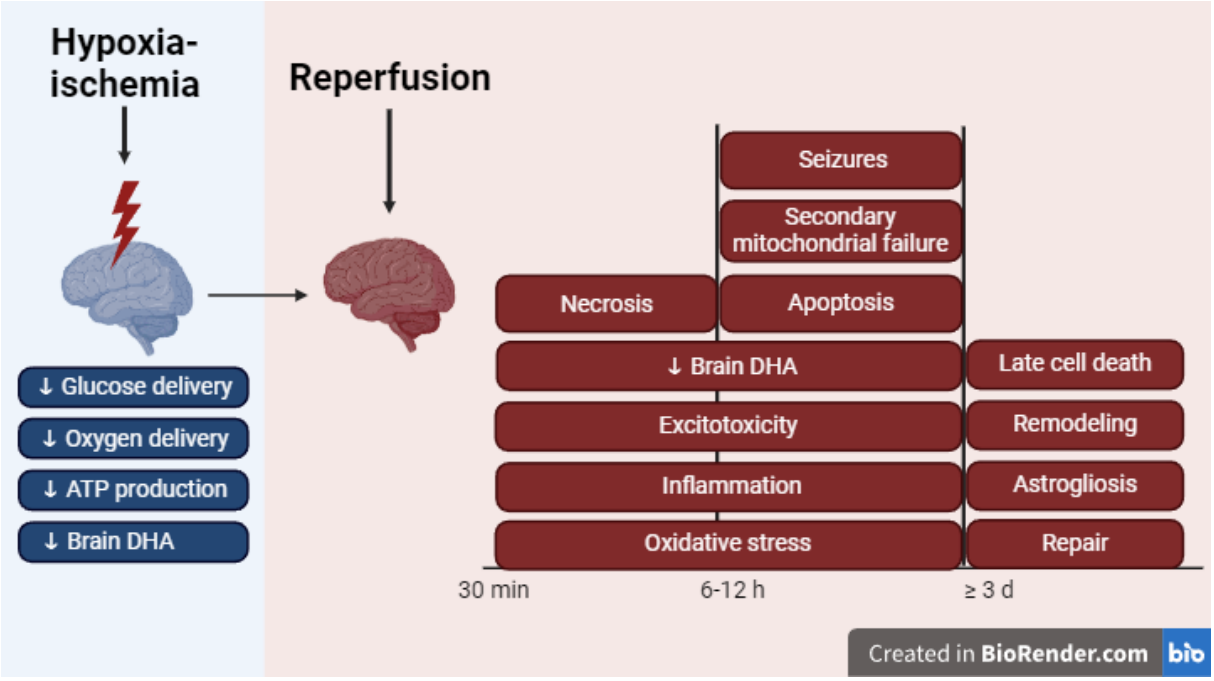

Fig 1. Pathophysiology after HI injury. Perinatal HI results in a decreased glucose and oxygen delivery, ATP production and DHA level in the brain. During reperfusion, excitotoxicity, inflammation, and oxidative stress cause cell death. On top of these events, seizures, a further decrease of DHA and secondary mitochondrial failure occur. After three days, the brain starts to remodel and repair itself, and astrogliosis takes place. Created with BioRender. Adjusted from Douglas-Escobar et al. (3).

One promising option in the treatment of HI injury is MSC therapy. MSCs are used for their capability to migrate to the site of injury and boost regeneration of neurons. This effect is believed to be exhibited by their secreted growth and trophic factors, for example brain-derived neurotrophic factor (BDNF), anti-inflammatory cytokines, and transforming growth factor (TGF) (19). Specifically in perinatal HI, MSCs and their secreting factors are able to promote the regenerative niche for the repair of brain damage (20). The past decade, MSCs have been proven safe and effective in reducing brain injury and improving cognitive and sensorimotor impairments in HI models (21,22). Currently, the approximate effectiveness of MSC therapy is 40% (19). At this moment, this effectiveness is promising enough to start several clinical trials to test MSC therapy in infants (23–27). Nevertheless, there is still room for improvement of this therapy. As MSCs can be given relatively late after injury maintaining their ability to activate regeneration, this leaves a window for a combination with other possible treatments (19,21).

A generally safe and easily implementable combination could involve a nutritional intervention. One such nutritional intervention is DHA, an omega-3 fatty acid that is highly associated with brain growth. Particularly in the cerebral cortex, DHA is incorporated in cell membranes and contributes to cognitive function (28). As brain DHA levels are affected by the pathophysiology of perinatal HI, restoring the DHA level in the brain could contribute to repairing HI injury. In previous DHA supplementation studies, researchers showed DHA protects against hippocampal loss, reduces grey and white matter injury, suppresses neuroinflammation, and limits neurological deficits (29,30). Specifically in perinatal HI mouse models, DHA supplementation has shown to improve memory and reduce lesion size, oxidative stress, and inflammation (13,31,32). Looking at these beneficial effects, DHA supplementation can potentially further optimise the current MSC therapy. In previous studies DHA supplementation is administered intraperitoneal (i.p.), whereas a diet with per os (p.o.) administration would be less invasive for the infants. Besides, these studies used free DHA, while only DHA bound to LPC is able to significantly increase the net amount of brain DHA (33). Therefore, p.o. LPC-DHA supplementation could have a more beneficial effect in restoring brain damage than the previously i.p. administered free DHA.

Hence, within this study, an orally administered LPC-DHA supplement was combined with MSC therapy in an *in vivo* model of perinatal HI to examine its potential effect on brain repair. Aside from *in vivo* experiments, DHA and LPC-DHA were used in *in vitro* hit models to examine the potential mechanisms by which they exhibit neuroprotective effects. By combining LPC-DHA with MSC therapy and unravelling its mechanism, the treatment options for infants suffering from HI injury are hopefully improved.

2. Materials and Methods

2.1 In vivo studies

To examine the effect of combining LPC-DHA with MSCs, an *in vivo* study was performed. Within this study, grey matter, white matter, and cortical organization was examined.

2.1.1 Animals

All procedures were performed in compliance with the Dutch and European international guidelines (Directive 86/609, ETS 123, Annex II) and approved by the Experimental Animal Committee Utrecht (Utrecht University, Utrecht, Netherlands) and the Central Authority for Scientific Procedures on Animals (The Hague, The Netherlands). Suffering of animals was minimized to the most feasible extent. Group sizes within this study (Table 2) are determined by the effect size of previous experiments and a performed power analysis.

2.1.2 Vannucci mouse model for perinatal HI (34)

C57Bl/6 mice (OlaHsa, ENVIGO, Horst, The Netherlands) were kept in standard housing conditions with food and water *ad libitum*. Breeding was performed by placing one wildtype male together with one or two females for 10 days. After 10 days of breeding, dams were housed separately to give birth to the pups. Litter size was controlled between 6-8 pups, to ensure adequate feeding of each pup. HI injury was induced in the pups at P9 by unilateral ligation of the carotid artery under isoflurane anaesthesia (5–10 minutes; 5% induction, 3–4% maintenance with flow O_2:air 1:1). For pre- and post-operative anaesthesia, Xylocaine (AstraZeneca, Cambridge, United Kingdom, N01BB02) and Bupivacaine (Actavis, currently Allergan Inc, Dublin, Ireland, N01BB01) were topically administered to the area of incision. Besides anaesthesia, a recovery period for rehabilitation was held in presence of the pup's mother for at least 75 minutes. Next, systemic hypoxia was induced for 45 minutes at 10% O_2 in a temperature-controlled hypoxic incubator. SHAM animals only received anaesthesia and a surgical incision without further interventions. Treatments were performed between P9 and P15 (Section 2.1.3. and 2.1.4). All mice were terminated at P37 and brains were perfused with 4% paraformaldehyde (PFA, VWR, Radnor, United States of America, VWRK4078.9020). After consecutive ethanol steps, brains were embedded in paraffin (SLEE medical, Nieder-Olm, Germany, 30010004) and stored until further analysis. The timeline of the *in vivo* experiment can be found in Fig 2.

2.1.3 Oral gavage with LPC-DHA

From P9 till P15, mice received a daily oral gavage with an in coconut oil (Merck KgA, Saint Louis, United States of America, C1758-500G) diluted LPC-DHA rich nutritional supplement (Lysoveta, Aker Biomarine, Oslo, Norway, Table 1) or only coconut oil (Merck KgA) as a vehicle. LPC-DHA (Aker Biomarine) was four times diluted coconut oil (Merck KgA) before administration. A final concentration of 5 µL LPC-DHA (Aker Biomarine) per gram of body weight was administered by an oral gavage with a sterile plastic feeding tube (22 ga, 38 mm, Instech Laboratories, Leipzich-Markkleeberg, Germany, FTP22-38), which was attached to a 25 µL Hamilton syringe (VWR, 549-0363). Administration was performed directly after induction of HI injury and all subsequent days until P15.

Table 1. Fatty acid profile of the LPC-DHA rich nutritional supplement Lysoveta

Fatty acid composition	Content in g/100 g
Total omega-3 fatty acids	30.42
C20:5 n-3 (EPA)	16.82
C22:6 n-3 (DHA)	9.29
Total LPC	41.69
EPA bound as LPC	13.02
DHA bound as LPC	7.40

2.1.4 Intranasal MSC treatment

At P12, mice received an intranasal administration of MSCs (GIBCO® C57BL/6 mouse, Thermo Fisher Scientific, Waltham, United States of America, S1502-100) in deionized phosphate-buffered saline (D-PBS, Merck KGaA, D8537) or only D-PBS (Merck KGaA) as a vehicle. MSCs (Thermo Fisher Scientific) were cryopreserved at passage 8 (P8) in vials containing $\geq$ 1 x 10^6 cells. Cells were thawed at P8 and cultured in T75 flasks (Corning Life Sciences, Corning, United States of America, 353110) with MSC medium consisting of DMEM:F12 GlutaMax (Thermo Fisher Scientific, 31331093), 10% fetal bovine serum (FBS, Thermo Fisher Scientific, 10270106), 0.05% gentamycin (Thermo Fisher Scientific, 15710064), and 1% penicillin/streptomycin (P/S, Thermo Fisher Scientific, 15140163). Cells were kept in a humidified incubator (PHCbi, Etten-Leur, The Netherlands, MCO-19M-PE) at 37 °C, 5% CO_2, and 90% humidity according to the manufacturer's protocol. MSCs (Thermo Fisher Scientific) were passaged once before administration. Before administration of the MSCs (Thermo Fisher Scientific), mice received an intranasal administration of hyaluronidase (100U, Merck KGaA) to increase permeability of the connective tissue in the nasal cavity. After 30 minutes, 0.5x10^6 MSCs (Thermo Fisher Scientific) in D-PBS (Merck KGaA) or only D-PBS (Merck KGaA) as a vehicle was administered intranasally. Administration was performed in three rounds with 2 droplets of 2 µL droplets per nostril.

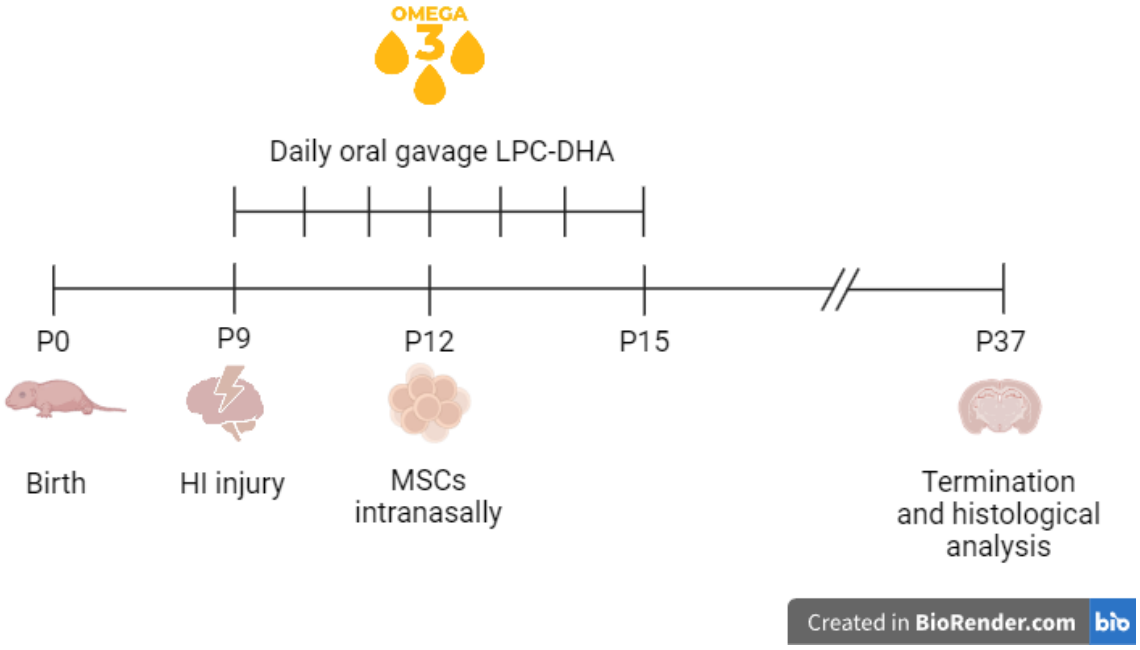

Figure 2. Timeline *in vivo* study performed in the Vannucci mouse model for perinatal HI. Mice are born at P0. HI injury is induced at P9. An LPC-DHA rich nutritional supplement is administered via oral gavage daily between P9-P15. MSCs are administered intranasally at P12. Mice are terminated at P37 and brains are used for histological analysis. Created with BioRender.com.

2.1.5 Immunohistochemistry

8 µm brain slices at bregma level -1.34 were obtained from the fixed brains by sectioning with a microtome (GMI Inc., Ramsey, United States of America, MICROM HM 355 S). From these slices, grey matter, white matter, and cortical organisation, were determined by staining for MAP2, MBP, and CTIP2, respectively. All antibodies used can be found in Table 3.

2.1.5.1 Grey matter

To determine grey matter loss, slides were deparaffinized and endogenous peroxidase was blocked with 3% H_2O_2 (VWR, 1.072.101.000) for 20 minutes. After blocking, slides were hydrated and antigen retrieval was performed in 10 mM citrate buffer (pH 6.0, Brunschwig Chemie, Amsterdam, The Netherlands, 2-3580.1) for 3 minutes at 95 °C. Slides were cooled on ice and washed with PBS (Invitrogen, Waltham, Unites States of America, 14200067). Aspecific binding of antibodies was blocked with 5% normal horse serum (NHS, Invitrogen, 26050088) in PBS (Invitrogen) for 30 minutes at 37 °C. Primary antibody (Merck KgA, M4403-2ML) in PBS (Invitrogen) with 2% NHS (Invitrogen) was incubated overnight. The next day, slides were washed with PBS (Invitrogen) and incubated with secondary antibody (Vector Laboratories, Newark, United States of America, BA-2000) in PBS (Invitrogen) for 45 minutes at 37 °C. After incubation, slides were washed in PBS (Invitrogen) and incubated with the standard peroxidase vectastain ABC kit (Vector Laboratories, PK-4000) for 30 minutes at RT. Subsequently, slides were washed in 0.05 M Tris-HCl (pH 7.6, Roche, Basel, Switzerland, 10708976001). Slides were incubated for 5 minutes in a solution of 3,3'-diaminobenzidine tetrahydrochloride (DAB, Merck KgA, D5637-10G) in 0.05M Tris-HCl (pH 7.6, Roche) with 30% H_2O_2 (VWR). Lastly, slides were dehydrated and embedded with DEPEX (Bioconnect, Huissen, the Netherlands, 18243.01). Images were taken at 2.5x magnification and analysed with Adobe Photoshop (Adobe, San Jose, United States of America, CS6). Ipsilateral hemispheric grey matter loss was calculated by (1- (MAP2+ area on the ipsilateral side / MAP2+ area on the contralateral side)) ×100.

2.1.5.2 White matter

To determine white matter loss, slides were deparaffinized and endogenous peroxidase was blocked with 3% H_2O_2 (VWR) for 20 minutes. After blocking, slides were hydrated and antigen retrieval was performed in 0.05M TRIS/0.01M EDTA buffer (pH 9, Roche, Merck KgA, 798681-1KG) for 15 minutes at 95 °C. Slides were cooled on ice and washed with 0.025% Triton (VWR, 1.086.031.000) in PBS (Invitrogen). Aspecific binding of antibodies was blocked with 20% normal goat serum (NGS, Vector Laboratories, S-1000-20) in PBS (Invitrogen) with 0.025% Triton (VWR) for 30 minutes at 37 °C. Next, slides were incubated with primary antibody (Abcam, Cambridge, United Kingdom, EPR21188) in PBS (Invitrogen) with 10% NGS (Vector Laboratories) and 0.025% Triton (VWR) overnight. The next day, slides were washed with PBS (Invitrogen) and incubated with secondary antibody (Vector Laboratories, BA-1000) in PBS (Invitrogen) for 45 minutes at 37 °C. After incubation, slides were washed in PBS (Invitrogen) with 0.025% Triton (VWR) and incubated with the standard peroxidase vectastain ABC kit (Vector Laboratories) for 30 minutes at RT. Subsequently, slides were washed in 0.05 M Tris-HCl (pH 7.6, Roche). Slides were incubated for 5 minutes in a solution of DAB (Merck KgA) in 0.05M Tris-HCl (pH 7.6, Roche) with 30% H_2O_2 (VWR). Lastly, slides were dehydrated and embedded with DEPEX (Bioconnect). Images were taken at 2.5x magnification and analysed with Fiji 1.53 (V&B) Software (National Institutes of Health and the Laboratory for Optical and Computational Instrumentation, Wisconsin, United States of America). Ipsilateral hemispheric white matter loss was calculated by (1- (MBP+ area on the ipsilateral side / MBP+ area on the contralateral side)) ×100.

2.1.5.3 Cortical organisation

In order to assess cortical organisation, slides were deparaffinized and hydrated. Antigen retrieval was performed in 10 mM citrate buffer (pH 6, Brunschwig Chemie) for 15 minutes at 95 °C. Slides were cooled on ice and permeabilized by washing in PBS (Invitrogen) with 0.05% Tween (VWR, 8.221.841.000). Aspecific binding of antibodies was inhibited by blocking with 5% normal donkey serum (NDS, Bioconnect, 017-000-121) in PBS (Invitrogen) with 0.05% Tween (VWR) for 30 minutes at RT. Primary antibody (Absolute antibody, Upper Heyford, United Kingdom, Ab00616-7.4) in PBS (Invitrogen) was incubated overnight at 4 °C. The next day, slides were washed in PBS (Invitrogen) and incubated with secondary antibody (Life Technologies, Carlsbad, Unites States of America, A-21209) in PBS (Invitrogen) for 75 minutes at RT. After incubation, slides were washed in PBS (Invitrogen) and incubated with DAPI (Merck, D9542) in demi water for 5 minutes at RT. Finally, slides were washed in demi water and embedded with FluorSave Reagent (Merck, 345789). CTIP2 stained slides were imaged using a fluorescence microscope (Carl Zeiss Microscopy, Oberkochen, Germany, Zeiss Axio Observer.Z1) equipped with an AxioCam camera (Carl Zeiss Microscopy, MR R3) and Zen2.3 software (Blue edition, Carl Zeiss Microscopy). 4 Separate images were taken of both ipsilateral and contralateral cortices at 2.5x magnification. Images were stitched and analysed using Fiji 1.53 (V&B) Software (National Institutes of Health and the Laboratory for Optical and Computational Instrumentation, Wisconsin, United States of America). Relative somatosensory cortex area was calculated by dividing the ipsilateral cortex area within a perimeter by the contralateral cortex area within a perimeter. Relative CTIP2+ area was calculated by dividing the ipsilateral layer V and VI CTIP2+ area within a perimeter corrected for the ipsilateral somatosensory cortex area by the contralateral layer V and VI CTIP2+ area within a perimeter corrected for the contralateral somatosensory cortex area. Relative CTIP2+ density was calculated by dividing the ipsilateral or contralateral CTIP2+ signal area within the layer V and VI CTIP2+ perimeter by its corresponding ipsilateral or contralateral somatosensory cortex area. Coronal sections of animals without a cortex were excluded from analysis (Table 2).

Table 2. Final number of animals per experimental group.

Group	Sex	Animals	Excluded grey matter	Excluded white matter	Excluded cortex area	Excluded layer V/VI	Excluded CTIP2 density
SHAM	m	12	1*	0	0	0	0
	f	12	0	0	0	0	0
Vehicle	m	15	0	0	1*	1*	1*
	f	9	0	0	1**	1**	1**
LPC-DHA	m	14	0	0	1*, 3**	3**	3**
	f	10	0	0	1*, 1**	1**	1**
MSCs	m	15	0	0	2**	2**	2**
	f	9	0	0	0	0	0
LPC-DHA + MSCs	m	13	1*	0	1**	1**	1**
	f	11	1*	0	2**	2**	2**

* Excluded by outlier test

** Excluded due to the lack of a cortex

Table 3. Antibodies used for *in vivo* stainings

Staining	Step	Antibody	Manufacturer	Catalogue number	Dilution
MAP2	Primary	Mouse anti-MAP2	Merck KgA	M4403-2ML	1:1000
	Secondary	Horse anti-mouse biotin	Vector Laboratories	BA-2000	1:100
MBP	Primary	Rabbit anti-MBP	Abcam	EPR21188	1:2000
	Secondary	Goat anti-rabbit biotin	Vector Laboratories	BA-1000	1:100
CTIP2	Primary	Rat monoclonal anti-CTIP2	Absolute antibody	Ab00616-7.4	1:1000
	Secondary	Donkey anti-rat AF594	Life Technologies	A-21209	1:500

2.2 *In vitro* hit models

To examine the mechanism by which DHA and LPC-DHA exhibit neuroprotective effects, different *in vitro* hit models were set up. These hit models address neuroinflammation, oxidative stress, DNA damage and OGD.

2.2.1 Primary microglia culture

A primary cortical microglia culture was isolated from a P1 C57BL/6 mouse (ENVIGO). Briefly, brains were dissected, and meninges were removed. Cortices were minced and incubated with 0.25% trypsin (Merck KgA, T4799) in Gey's balanced salt solution (GBSS, Merck KgA, G9779-500mL) supplemented with 1% P/S (Thermo Fisher Scientific, 15140122) and 30 mM D-(+)-glucose (Merck KgA, G7021) for 15 minutes. After incubation, cells were resuspended until a homogenous suspension was formed. T75 flasks (Corning Life Sciences) were coated with poly-L-ornithine (PLO, Merck KgA, P3655). Microglia yield of 1 animal was cultured in 1 PLO-coated T75 flask (Merck KgA, Corning Life Sciences) with DMEM (Thermo Fisher Scientific, 41965-039) supplemented with HamF10 (Thermo Fisher Scientific, 31550-023), 10% FBS (Invitrogen, 10270106), 1:100 P/S (Thermo Fisher Scientific, 15140122), and 1:100 glutamine (Invitrogen, 25030024) in a humidified incubator (PHCbi) with 5% CO_2 level at 37 °C. After 10–12 days of culture, microglia were detached by shaking the flasks for 20-22 h at 130-135 rpm and 37°C. Following, microglia were centrifuged for 10 minutes at 120 rpm at RT to be collected.

2.2.1.1 Neuroinflammation model

Primary microglia were plated in a PLO-coated 24-wells plate (Merck KgA, Corning Life Sciences, 3524) with 15×10^5 microglia/well and were allowed to attach for 24 h. The next day, microglia were hit with lipopolysaccharide (LPS, Merck KgA, L4516-1MG) and exposed to 4, 20, 50 or 100 µM DHA (Merck KgA, D2534) in PBS (Invitrogen) with 1% Bovine Serum Albumin (BSA, Merck KgA, A9647-10G) for 24 hours. Control medium was corrected for BSA exposure at the 20 µM level, resulting in final concentrations of 0.02% BSA (Merck KgA) in the plate. After incubation, the supernatant was collected and stored at -80 °C until analysis. Supernatant was examined by a tumor necrosis factor alpha (TNF-α) ELISA (Ucytech, Utrecht, The Netherlands, CT303A) according to the manufacturer's protocol.

2.2.2 SH-SY5Y culture

The human neuroblastoma cell line SH-SY5Y (ATCC, Manassas, United States of America, CRL-2266) was cultured in DMEM/F12 medium (Thermo Fisher Scientific, 11330057) supplemented with 10% FBS (Invitrogen) and 1:100 P/S (Thermo Fisher Scientific). Cells were grown in T75 flasks (Corning Life Sciences) in a humidified incubator (PHCbi) with 5% CO_2 at 37 °C. SH-SY5Y cells were harvested by incubation in trypsin-EDTA (Invitrogen, 25300-054) for 2 minutes. Following, cells were centrifuged for 5 minutes at 300 rpm at RT to be collected.

2.2.2.1 Oxidative stress model

SH-SY5Y cells (ATCC) were plated in a 96-wells plate (Thermo Fisher Scientific, 167008) with 6×10^4 cells/well and were allowed to attach overnight. The next day, cells were incubated with 60 µM H_2O_2 (VWR) or control medium and 0, 5, 10, 25 or 50 µM DHA (Merck KgA) in PBS (Invitrogen) with 1% BSA (Merck KgA) or LPC-DHA (Aker Biomarine) in 0.7% dimethyl sulfoxide (DMSO, Duchefa Farma, Haarlem, The Netherlands, D1370.0100) in a humidified incubator (PHCbi) with 5% CO_2 at 37 °C for 24 hours. Control medium was corrected for BSA and DMSO exposure at the 25 µM level, resulting in final concentrations of 0.025% BSA (Merck KgA) or 0.0175% DMSO (Duchefa Farma) in the plate for DHA (Merck KgA) and LPC-DHA (Aker Biomarine), respectively. Neuronal cell death was assessed with a 3-(4,5-dimethylthiazol-2-yl)-2,5-diphenyl-2H-tetrazolium bromide (MTT) assay (Section 2.2.3).

2.2.2.2 DNA damage model

SH-SY5Y cells (ATCC) were plated in a 96-wells plate (Thermo Fisher Scientific) with 6×10^4 cells/well and were allowed to attach overnight. The next day, cells were incubated with 2800 nM etoposide (Merck KgA, E1383-25MG) or control medium and 0, 5, 10, 25 or 50 µM DHA (Merck KgA) in 1% BSA (Merck KgA) or LPC-DHA (Aker Biomarine) in 0.7% DMSO (Duchefa Farma) in a humidified incubator (PHCbi) with 5% CO_2 at 37 °C for 24 hours. Control medium was corrected for BSA and DMSO exposure at the 25 µM level, resulting in final concentrations of 0.025% BSA (Merck KgA) or 0.0175% DMSO (Duchefa Farma) in the plate for DHA (Merck KgA) and LPC-DHA (Aker Biomarine), respectively. Neuronal cell death was assessed with an MTT assay (Section 2.2.3).

2.2.2.3 OGD model

SH-SY5Y cells (ATCC) were plated in a 96-wells plate (Thermo Fisher Scientific) with 6×10^4 cells/well and were allowed to attach overnight. The next day, culture medium was replaced by DMEM without glucose (Merck KgA, 11966025) supplemented with 1:100 P/S (Thermo Fisher Scientific, 15140122) and 0, 5, 10, 25 or 50 µM DHA (Merck KgA) in 1% BSA (Merck KgA) or LPC-DHA (Aker Biomarine) in 0.7% DMSO (Duchefa Farma). Cells were incubated in a humidified hypoxic incubator with 1% O_2 and 5% CO_2 at 37 °C (PHCbi, Cell-IQ 5.7 cu.ft. Multigas CO_2/O_2 Incubator MCO-170MP-PA) for 24 h. In parallel, a control plate was incubated with culturing medium in a humidified normoxic incubator (PHCbi) with 21% O_2 and 5% CO_2 at 37 °C for 24 h. Control medium was corrected for BSA and DMSO exposure at the 25 µM level, resulting in final concentrations of 0.025% BSA (Merck KgA) or 0.0175% DMSO (Duchefa Farma) in the plate for DHA (Merck KgA) and LPC-DHA (Aker Biomarine), respectively. Neuronal cell death was assessed with an MTT assay (Section 2.2.3).

2.2.3 MTT assay

After exposure within the oxidative stress, DNA damage, and OGD model (Section 2.2.2.1, 2.2.2.2, and 2.2.2.3), hit medium was replaced by culture medium containing 0.5 mg/ml MTT (Merck KgA, M2128-250MG) in PBS (Invitrogen). MTT solution was incubated for 3 h in a humidified incubator (PHCbi) with 5% CO_2 at 37 °C. After incubation, medium was removed from the wells and MTT crystals were dissolved in 100 µL DMSO (VWR, 23500260). Optical density was measured at 570 nm using a spectrophotometer (Thermo Fisher Scientific, Multiskan GO).

2.3 Statistical analysis

All data was acquired being blinded. Statistical analysis was performed using GraphPad Prism 8.3 (GraphPad Software, Dotmatics, Boston, United States of America). Outliers were identified by the ROUT analysis (Q = 1%). Data was checked for normal (Gaussian) distribution using the Shapiro-Wilk normality test. If data was normally distributed, statistical analysis was performed by a one-way ANOVA with Holm-Šidák post-hoc tests. If data was not normally distributed, statistical analysis was performed by a nonparametric test with Dunn's post-hoc tests. Data is presented as the mean ± SEM. Differences of $p \leq 0.05$ were considered statistically significant.

3. Results

3.1 *In vivo* results

3.1.1 A combined treatment with LPC-DHA and MSCs reduces grey matter loss after HI injury

In order to examine grey matter loss in the HI injured animals, coronal sections were stained for MAP2 and the percentage of ipsilateral hemispheric neuronal loss was determined. After quantification, HI animals have approximately 30% ipsilateral grey matter loss ($p<0.0001$, Fig 3A-B). Grey matter loss is not reduced after treatment with LPC-DHA or MSCs alone compared to non-treated controls ($p=0.1225$, $p=0.1225$, Fig 3A-B). However, after a combined treatment with LPC-DHA and MSCs, grey matter loss is significantly reduced compared to non-treated controls ($p=0.0041$, Fig 3A-B).

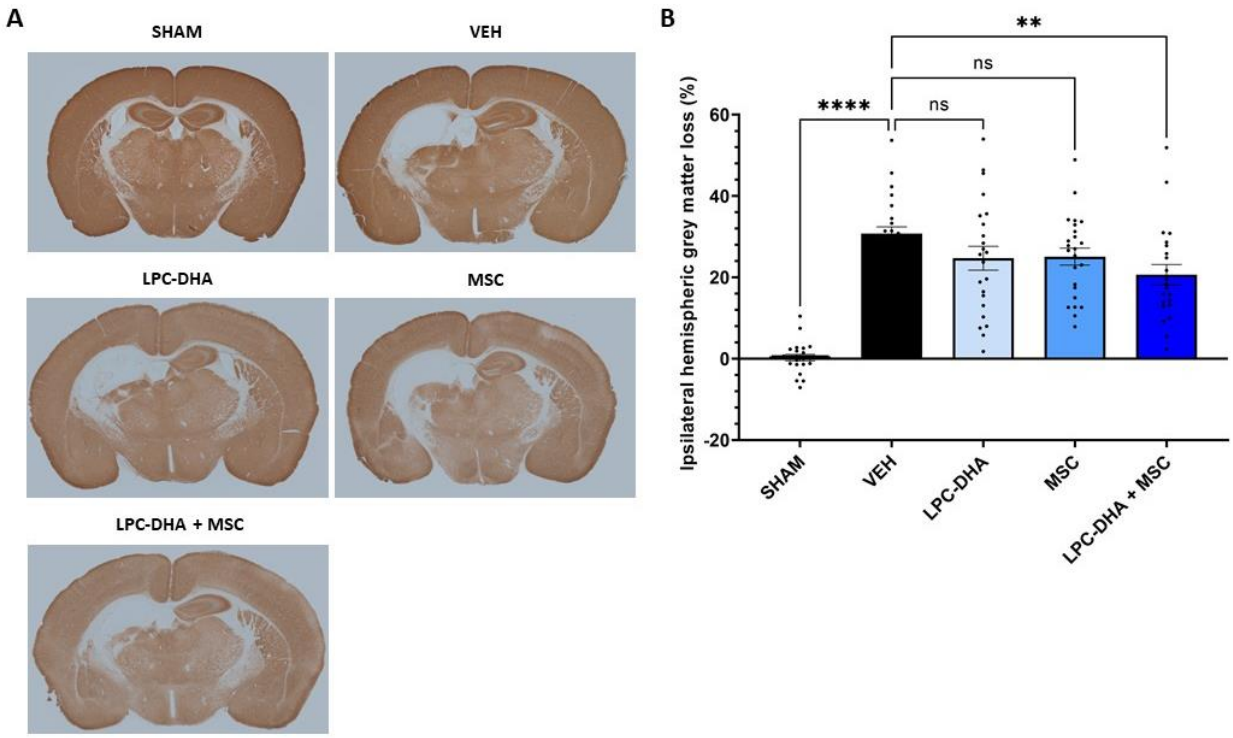

Fig 3. Ipsilateral hemispheric grey matter loss after HI injury in MAP2 stained coronal sections. A) Representative images of MAP2 staining per treatment group (2.5x magnification). B) Quantification of ipsilateral hemispheric grey matter loss. SHAM, n=23; VEH, n=24; LPC-DHA, n=24; MSC, n=24; LPC-DHA + MSC, n=22. VEH = vehicle treated animals. ** p<0.01. **** p<0.0001. Data represents mean + SEM.

3.1.2 LPC-DHA, MSC and combined LPC-DHA and MSC treatments do not reduce myelin loss after HI injury

In order to examine loss of myelin content in HI injured animals, coronal sections were stained for MBP and the percentage of ipsilateral hemispheric myelin loss was determined. HI injured animals have approximately 30% ipsilateral myelin loss ($p<0.0001$, Fig 4A-B). LPC-DHA, MSCs, and LPC-DHA with MSC treatment do not significantly decrease myelin loss compared to non-treated controls ($p=0.7507$, $p=0.7507$, $p=0.6539$, Fig 4A-B).

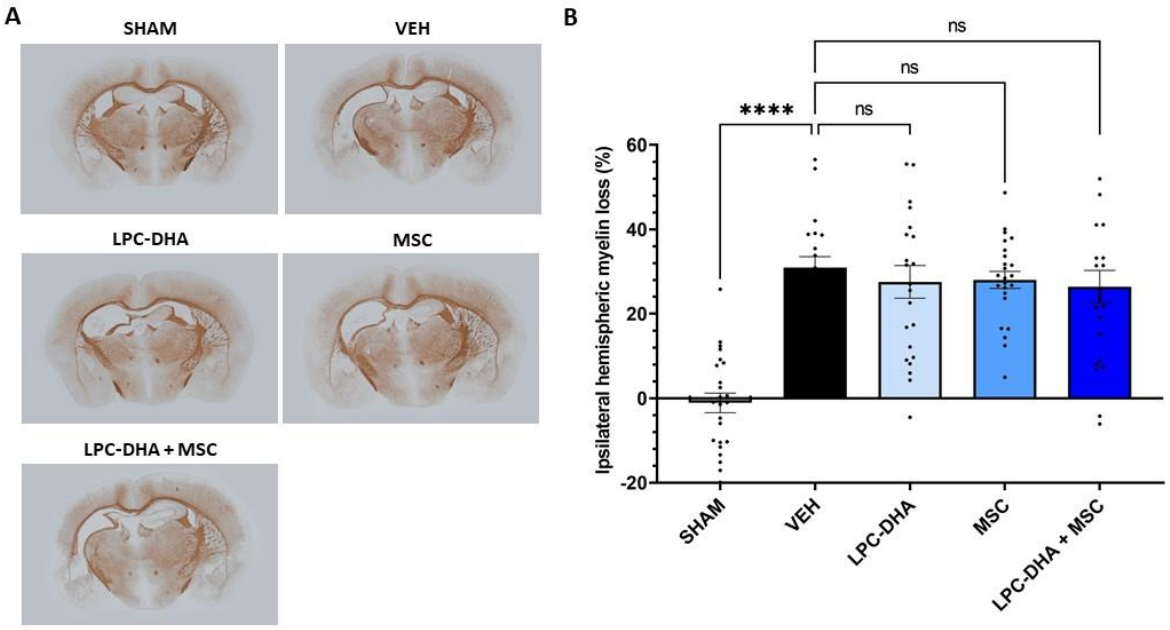

Fig 4. Ipsilateral hemispheric myelin loss after HI injury in MBP stained coronal sections. A) Representative images of MBP staining per treatment group (2.5x magnification). B) Quantification of ipsilateral hemispheric myelin loss at bregma level -1.34. SHAM, n=24; VEH, n=24; LPC-DHA, n=24; MSC, n=24; LPC-DHA + MSC, n=24. VEH = vehicle treated animals. **** $p<0.0001$. Data represents mean + SEM.

3.1.3 Relative area of the ipsilateral somatosensory cortex shrinks after HI injury *in vivo*

The somatosensory cortex is often injured after HI injury (20,35). To further examine the effect of our treatment on the somatosensory cortex, its relative area was determined. Representative images per group at 2.5x magnification show cortical lamination (Fig 5A). After HI injury, the somatosensory cortex area decreases ($p<0.0001$, Fig 5B). After treatments with LPC-DHA, MSCs or LPC-DHA with MSCs the somatosensory cortex area did not significantly increase compared to non-treated controls ($p=0.2060$, $p=0.9112$, $p= 0.0721$, Fig 5B). Noteworthy, our combined treatment of LPC-DHA with MSCs shows a trend towards somatosensory cortex area restoration ($p=0.0721$, Fig 5B).

3.1.4 Relative area of layer V and VI does not differ after HI injury *in vivo*

In order to determine if the size of all layers of the somatosensory cortex decrease relatively, the CTIP2+ stained area in the deeper layers of the somatosensory cortex was quantified. This measurement reflects the relative area of layer V and VI within the somatosensory cortex. Even though the total somatosensory cortex area decreased after HI injury ($p<0.0001$, Fig 5B), the relative CTIP2+ area stayed equal after HI injury ($p=0.9922$, Fig 5C). Moreover, none of the proposed treatments with LPC-DHA, MSCs or LPC-DHA with MSCs changed the relative CTIP2+ area compared to non-treated controls ($p=0.9922$, $p=0.8673$, $p=0.9922$, Fig 5C).

3.1.5 The relatively increased neuronal density on the ipsilateral side within layer V and VI of the somatosensory after HI injury *in vivo* is compensated on the contralateral side by a combined treatment of DHA and MSCs

Although the area within the perimeter of layer V and VI did not change, cell density could be altered. The relative CTIP2+ signal area within layer V and VI increases on the ipsilateral side after HI injury ($p=0.0065$, Fig 5D), indicating a higher density of CTIP2+ cells in layer V and VI. Treatment with LPC-DHA or MSCs alone did not change the increased CTIP2+ density on the ipsilateral side ($p<0.0001$, $p=0.0015$, Fig 5D). After treatment with the combination of LPC-DHA and MSCs, the relative CTIP2+ density is similar between the ipsilateral and contralateral side ($p=0.0935$, Fig 5D). Though, this restored balance is rather due to a compensation on the contralateral side than a decrease of the ipsilateral side.

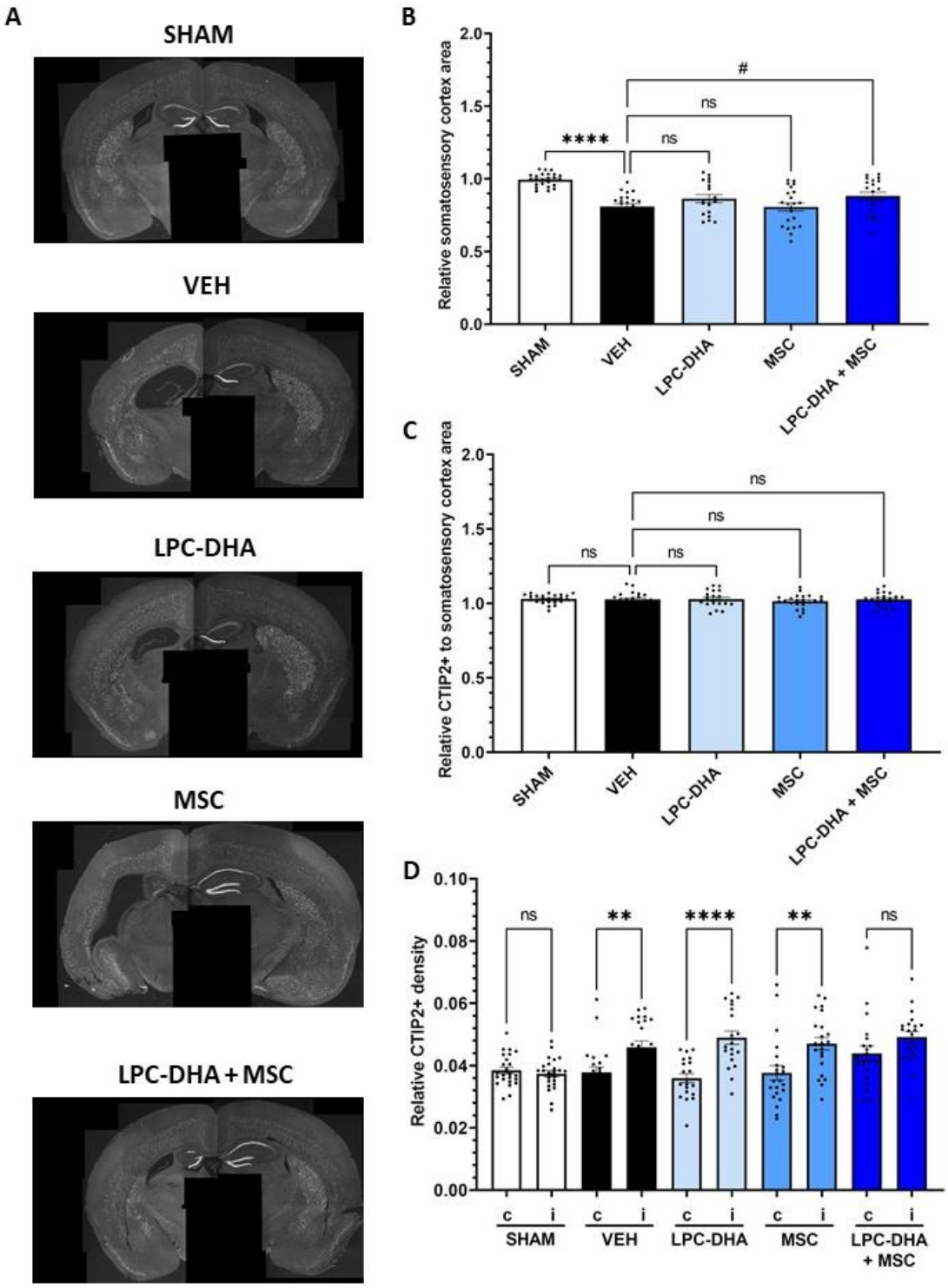

Fig 5. Cortical organization after HI injury in CTIP2 stained coronal sections. A) Representative images of CTIP2 staining per treatment group (2.5x magnification). B) Quantification of relative somatosensory cortex area at bregma -1.34. SHAM, n=24; VEH, n=22; LPC-DHA, n=18; MSC, n=22; LPC-DHA + MSC, n=21. C) Quantification of relative CTIP2+ area within the somatosensory cortex area. SHAM, n=24; VEH, n=22; LPC-DHA, n=20; MSC, n=22; LPC-DHA + MSC, n=21. D) Quantification of relative CTIP2+ density in the CTIP2+ perimeter. SHAM, n=24; VEH, n=22; LPC-DHA, n=20; MSC, n=22; LPC-DHA+ MSC, n=21. VEH = vehicle treated animals; c = contralateral; i = ipsilateral. # $p<0.1$. ** $p<0.01$. *** $p<0.001$. **** $p<0.0001$. Data represents mean + SEM.

3.2 *In vitro results*

3.2.1 DHA dose dependently decreases TNF-α production *in vitro* after LPS induced neuroinflammation in primary microglia

To dive deeper into the working mechanisms of DHA, the ability of DHA to suppress neuroinflammation was assessed in a microglia LPS hit model. LPS is known to induce inflammation and increase TNF-α production by primary microglia (36). When DHA was added in doses of 4, 20, 50 and 100 µM, TNF-α production was dose dependently reduced compared to non-treated microglia (p=0.0032, p=0.0014, p=0.0005, p=0.0005, Fig 6). This indicates DHA is able to reduce the neuroinflammatory response of microglia to an inflammatory hit.

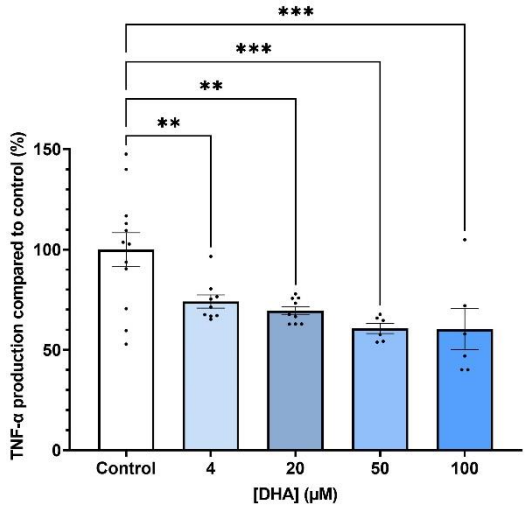

Fig 6. TNF-α production by primary microglia after LPS stimulation and DHA treatment compared to control. Control, n=12; 4 µM, n=6; 20 µM, n=6; 50 µM, n=6; 100 µM, n=6. ** p<0.01. *** p<0.001. Data represents mean + SEM.

3.2.2 Both DHA and LPC-DHA increase neuronal cell viability in *vitro*

To examine differential effects of DHA and LPC-DHA on neuronal cell viability, a SH-SY5Y cell culture was used. Cell viability of SH-SY5Y cells dose dependently increases after DHA and LPC-DHA exposure (Fig 7). A significant increase in cell viability was noted after exposure to both 10 and 25 µM DHA (p=0.0070, p=0.0065, Fig 7A), and 10 µM LPC-DHA compared to non-treated cells (p=0.0142, Fig 7B). The positive effect of DHA and LPC-DHA on cell viability was lost at 50 µM (0.5502, Fig 7A) and 25 µM (p=0.3153, Fig 7B), respectively. Significant toxic effects can be seen at 50 µM LPC-DHA (p=0.0010, Fig 7B). All in all, both DHA and LPC-DHA are able to increase neuronal cell viability.

3.2.3 DHA and LPC-DHA prevent neuronal cell death by H_2O_2 induced oxidative stress *in vitro*

The ability of DHA and LPC-DHA to rescue neurons after oxidative stress was examined with a neuronal H_2O_2 hit model. 60 µM H_2O_2 was determined to be the optimal dose in our hit model (Supplementary Fig S1). Both DHA and LPC-DHA dose dependently protect neuronal cell viability after a hit with 60 µM H_2O_2 (Fig 8). A significant increase in neuronal cell viability was seen at 10 µM DHA (p=0.0073, Fig 8A) and LPC-DHA compared to non-treated cells (p=0.0195, Fig 8B). Again, significant toxic effects are reached at 50 µM LPC-DHA (p<0.0001, Fig 8B). Concluding, DHA and LPC-DHA seem to have similar neuroprotective effect on neuronal cell culture viability after a H_2O_2 induced oxidative stress hit.

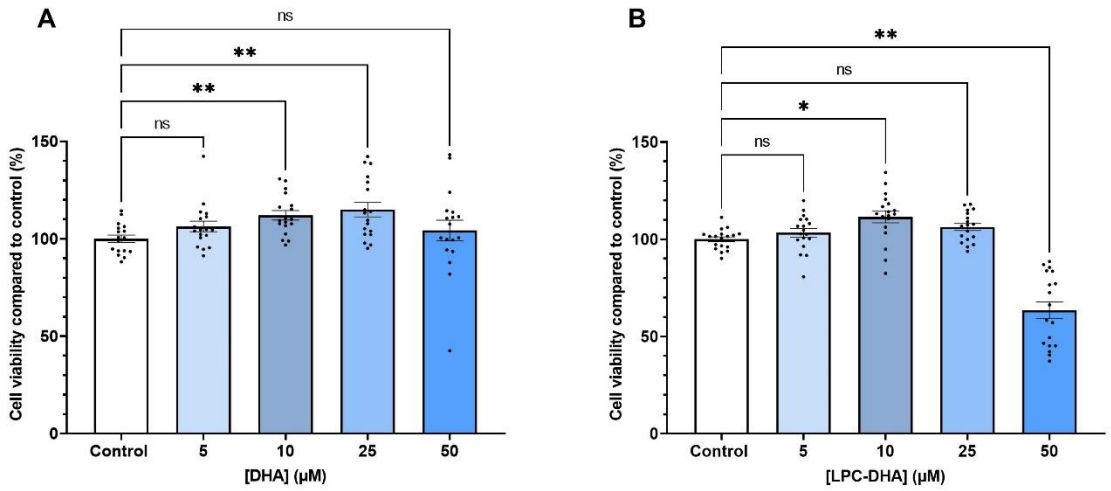

Fig 7. Neuronal cell viability after DHA and LPC-DHA treatment A) Neuronal cell viability after treatment with a range of DHA concentrations. Control, n=17; 5 µM, n=18; 10 µM, n=18; 25 µM, n=18; 50 µM, n=18. B) Neuronal cell viability after treatment with a range of LPC-DHA concentrations. Control, n=18; 5 µM, n=18; 10 µM, n=18; 25 µM, n=18; 50 µM, n=18. * p<0.05. ** p<0.01. Data represents mean + SEM.

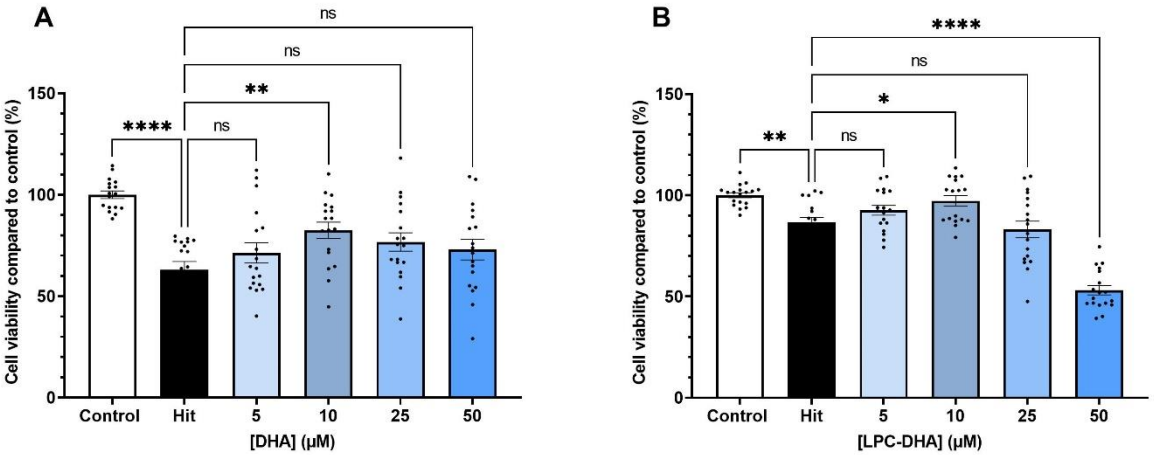

Fig 8. Neuronal cell viability after H_2O_2 induced oxidative stress and DHA or LPC-DHA treatment. A) Neuronal cell viability after treatment with a range of DHA concentrations. Control, n=17; Hit, n=17; 5 µM, n=18; 10 µM, n=18; 25 µM, n=18; 50 µM, n=18. B) Neuronal cell viability after treatment with a range of LPC-DHA concentrations. Control, n=18; Hit, n=18; 5 µM, n=18; 10 µM, n=17; 25 µM, n=18; 50 µM, n=18. * p<0.05. ** p<0.01. **** p<0.0001. Data represents mean + SEM.

3.2.4 Both DHA and LPC-DHA do not prevent neuronal cell death after etoposide-induced DNA damage *in vitro*

In order to validate if the protective effects of DHA and LPC-DHA work specifically on oxidative stress, an *in vitro* neuronal etoposide hit model was established. 2800 nM etoposide was determined to be the optimal dose in our hit model (Supplementary Fig S2). DHA did not rescue the neurons at 5, 10, or 25 µM compared to non-treated cells ($p=0.3431$, $p=0.7320$, $p=0.3431$, Fig 9A). 50 µM DHA even showed toxic effects and decreased the neuronal cell viability further ($p=0.0085$, Fig 8A). LPC-DHA was also not able to rescue the neurons at 5 µM LPC-DHA compared to non-treated cells ($p=0.5207$, Fig 9B). Toxic effects were shown at 10, 25 and 50 µM LPC-DHA ($p=0.0103$, $p<0.0001$, $p<0.0001$, Fig 9B). As seen in the *in vitro* model without a hit and the oxidative stress model, LPC-DHA seems more toxic than DHA (Fig 7A-B, Fig 8A-B). The inability to rescue neurons in the DNA damage model, implicates DHA and LPC-DHA most likely work specifically against oxidative stress.

3.2.5 DHA prevents and LPC-DHA increases neuronal cell death after an *in vitro* OGD hit

As neurons were protected from oxidative stress, but not from DNA damage by DHA or LPC-DHA treatment, a more translational neuronal OGD model was established to further unravel the neuroprotective mechanisms of DHA and LPC-DHA after HI jury. Optimal OGD exposure was determined to be 24 hours (Supplementary Fig S3). The OGD hit decreases cell viability with approximately 30% ($p<0.0001$, Fig 10). Cell viability is significantly increased after a treatment with 10 µM DHA compared to non-treated cells ($p=0.0182$, Fig 10A), which is in line with our findings in the oxidative stress model (Fig 8A). DHA has a dose dependent beneficial effect after the OGD hit (Fig 10A). On the contrary, LPC-DHA treatment with 5, 10, 25 or 50 µM dose dependently decreases cell viability after an OGD hit ($p<0.0001$, $p<0.0001$, $p<0.0001$, $p<0.0001$, Fig 10B). These toxic effects are harsher than previously found in the DNA damage model (Fig 9B). Concluding, DHA and LPC-DHA seem to have radical scavenging properties, but exhibit different effects when excitotoxicity and inflammation engage in an *in vitro* setting.

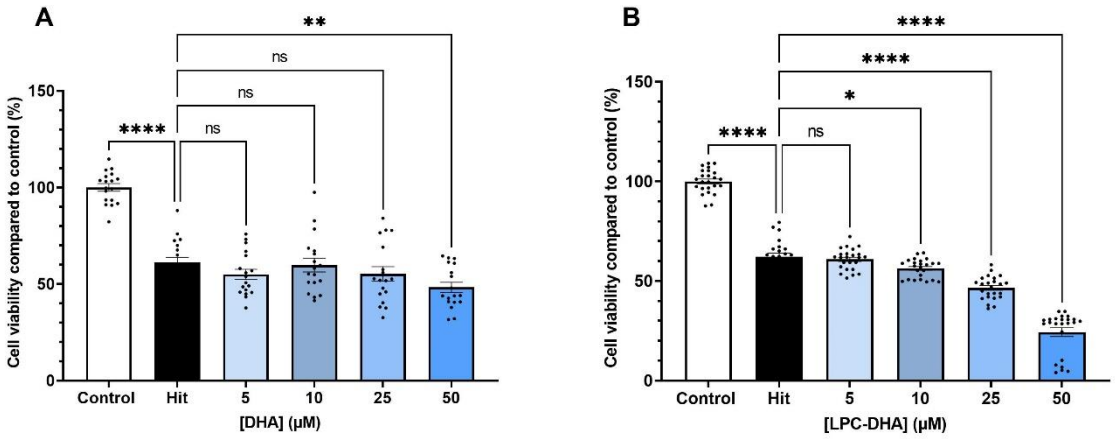

Fig 9. Neuronal cell viability after etoposide-induced DNA damage and DHA or LPC-DHA treatment. A) Neuronal cell viability after treatment with a range of DHA concentrations. Control, n=18; Hit, n=18; 5 µM, n=18; 10 µM, n=18; 25 µM, n=18; 50 µM, n=18. B) Neuronal cell viability after treatment with a range of LPC-DHA concentrations. Control, n=18; Hit, n=18; 5 µM, n=18; 10 µM, n=18; 25 µM, n=18; 50 µM, n=18. * p<0.05. ** p<0.01. **** p<0.0001. Data represents mean + SEM.

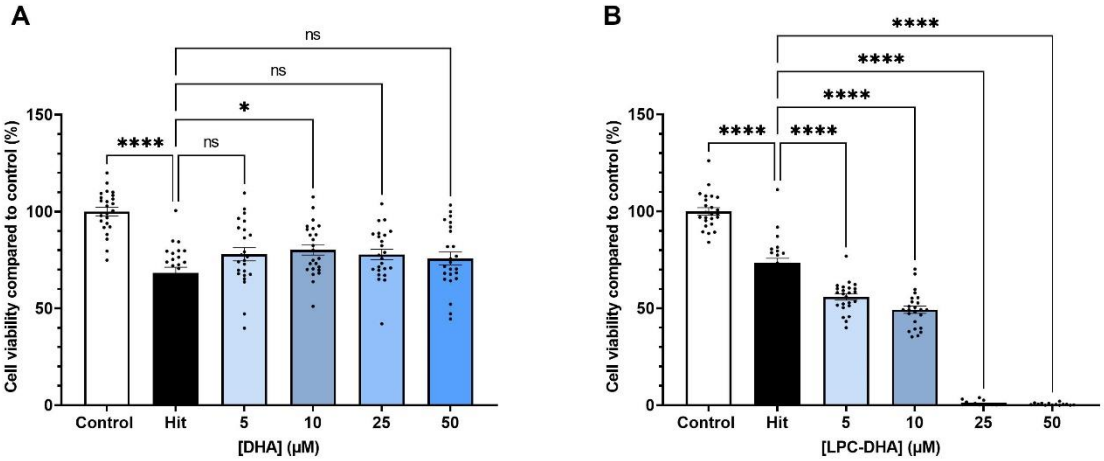

Fig 10. Neuronal cell viability after deprivation of oxygen and glucose and DHA or LPC-DHA treatment. A) Neuronal cell viability after treatment with a range of DHA concentrations. Control, n=24; Hit, n=24; 5 µM, n=24; 10 µM, n=24; 25 µM, n=24; 50 µM, n=24. B) Neuronal cell viability after treatment with a range of LPC-DHA concentrations. Control, n=24; Hit, n=24; 5 µM, n=24; 10 µM, n=24; 25 µM, n=24; 50 µM, n=24. * p<0.05. **** p<0.0001. Data represents mean + SEM.

4. Discussion

Within this study, the brain restoring effect of combining LPC-DHA with MSC therapy for the treatment of perinatal HI *in vivo* and the potential neuroprotective mechanism of DHA and LPC-DHA after injury *in vitro* have been studied.

Within our *in vivo* model the grey matter hemispheric loss was assessed by staining for MAP2. MAP2 is a neuronal protein expressed by the cytoskeleton and accordingly a marker for grey matter (37). In our data, vehicle treated HI injured animals have an ipsilateral grey matter loss of approximately 30%, which is in line with previous research (22,38). The HI injury is mainly affecting the hippocampus, which is involved in spatial memory and learning abilities (39). This study is the first to show that short term treatment with LPC-DHA and MSCs decreases grey matter loss after HI injury, while MSCs or LPC-DHA alone were not able to decrease grey matter loss. This enhanced efficacy of combining MSCs and LPC-DHA could possibly result from a reduction in neuroinflammation and the neuroprotection against ROS.

Our *in vitro* experiments and literature confirmed DHA's mechanism of action involves the reduction of the pro-inflammatory cytokine TNF-α (36). Together with MSCs being able to excrete anti-inflammatory cytokines and their inhibitory effect on microglia activation and astrocytosis, the LPC-DHA might contribute alongside the MSCs to a neuroprotective environment beneficial to neuronal regeneration (19). To further confirm this hypothesis, future research should examine if LPC-DHA exerts the same TNF-α suppressing effect as DHA showed *in vitro*. Besides, neuroinflammation should be assessed shortly after the combined treatment of LPC-DHA and MSCs *in vivo* to confirm the proposed involvement of an anti-inflammatory mechanism.

Next, combined data of our *in vitro* experiments and literature show DHA and LPC-DHA similarly protect neurons from ROS induced cell death (40,41). This study is the first to test LPC-DHA's capacity in protecting neurons from oxidative stress. The observed reduction of oxidative stress by LPC-DHA can create a neuroprotective environment contributing to the MSCs boosting neurogenesis in parallel. This increased neuroprotection and neurogenesis can play a role in limiting grey matter loss seen by the combined treatment with MSCs and LPC-DHA. To confirm a treatment with LPC-DHA and MSCs limits oxidative stress after HI injury, an *in vivo* study should be performed exploring the proposed involvement of oxidative stress pathways. To specifically confirm the mechanism by which LPC-DHA reduces oxidative stress is likewise DHA's action, which includes reducing the numbers of radicals, LPC-DHA should also be studied for its capacity to decrease the number of radicals during future *in vitro* experiments (41).

The effects of DHA and LPC-DHA seem to point specifically towards anti-oxidative stress and anti-inflammatory pathways as our study shows that DHA and LPC-DHA do not protect the cells from etoposide-induced DNA damage. In line with this, DHA has been shown to decrease DNA repairing gene expression (42). To confirm DHA and LPC-DHA indeed limit inflammation and oxidative stress in a more translational *in vitro* setting, injury was induced in an OGD model. OGD induces a combination of inflammation, ROS and excitotoxicity (3,43–45). Our experiments and literature shows DHA protects neurons after an OGD hit (41,46). This study was the first to study LPC-DHA in an *in vitro* OGD model and found it did not protect the neurons in the current setup. Moreover, clear toxic effects of LPC-DHA could be observed in the OGD hit model. These toxic effects can be explained by the fact that LPC-DHA has an amphiphilic nature and can interfere with membranes. The LPC component on its own is known to integrate in the membrane causing a higher membrane permeability (47). LPC's detergent action can result into cell lysis in an *in vitro* setting. It is known albumin, which is known to be important in LPC-DHA transport *in vivo*, can prevent LPC's detergent action and even contribute to neuroprotection

(48,49). Albumin was present in our *in vivo* study and *in vitro* experiments with DHA, but not in our *in vitro* experiments with LPC-DHA. In future *in vitro* experiments, addition of albumin might prevent LPC-DHA's detergent action and give new insights in the potential neuroprotective effect of LPC-DHA exhibited *in vivo*. Adding, the effect of DHA and LPC-DHA on neuroinflammation and ROS were examined separately in this study, but the excitotoxicity component within the OGD model is not yet examined separately. Excitotoxicity can be modelled in the SH-SY5Y cell line and examination of DHA and LPC-DHA's protective effects within this model could potentially also give even more specific insights into the involved pathways after LPC-DHA treatment (50).

Apart from grey matter injury, white matter injury was also assessed in this study by a MBP staining. MBP is a protein expressed through the myelin sheet and accordingly a marker for white matter (51). In line with previous research, white matter was reduced with approximately 30% after HI injury (52,53). Myelin is important in signal transduction and therefore a reduction in myelin results in cognitive difficulties and motor abnormalities (54). Though, none of our treatments reduced the myelin loss. Studies within our lab show it should be possible to reduce myelin loss after HI injury with MSCs (22). At this moment, only one dose and timing of LPC-DHA and MSCs is tested, which might not yet be optimal. Therefore, optimal dose and timing studies need to be performed to claim with certainty whether a combined treatment of LPC-DHA and MSCs is also able to boost myelination.

Our last *in vivo* assessment involved the cortical organization by staining our coronal sections for CTIP2. CTIP2 is a specific marker for pyramidal neurons mainly residing in layer V and VI of the cortex. This study is the first to examine the somatosensory cortex and its specific deeper layers after HI injury at term equivalent age in mice. The only other available literature on cortical organization in mice includes two studies of injury at preterm equivalent age (52,55). Both our study and the study of Shinoyama et al., found the somatosensory cortex shrinks after HI injury, which indicates not only the hippocampus, but also the cortex gets affected by HI injury (55). At this moment, LPC-DHA, MSCs or the combined treatment with LPC-DHA and MSCs were not able to restore the somatosensory cortex area. Though, our combined treatment with LPC-DHA and MSCs shows a potential in somatosensory cortex restoration after optimization of the treatment. Future studies could focus on more specifically targeting the cortex after HI injury.

The somatosensory cortex consists of multiple layers and develops from an inside out manner (56). Interestingly, our study showed not all cortical layers shrink equally. The deeper layers are not affected after HI injury in our at term equivalent age model, whereas these layers were affected in a preterm equivalent age model (52). This difference can be explained by the timepoint of HI induction and the development of the cortex. Between P7 and P10, pyramidal neurons, mainly residing in the deeper layers of the cortex, are in a developmental stage where they largely increase in complexity (57). The more robust deeper layer neurons in the term equivalent age model could therefore be more resistant than the undeveloped deeper layer neurons in the preterm equivalent age model.

Although the total deeper layer size was protected, an increased density of CTIP2+ pyramidal neurons was observed after HI injury. The increased pyramidal neuron density on the ipsilateral side after HI injury can be explained by the increased proliferation of pyramidal neurons after ischemia, which has also been found in rat models with HI at adult equivalent age (58,59). The increased proliferation on the contralateral side most likely results from the LPC-DHA component within our treatment. MSCs are known to migrate to the site of injury where they boost proliferation and promote differentiation towards neurons (19,60). Therefore, it is hypothesized mainly LPC-DHA would increase pyramidal neuron proliferation on the contralateral side to compensate for the increased pyramidal neuron proliferation on the ipsilateral side. This would indicate LPC-DHA and MSCs have distinct proliferative functions and work in parallel. Future studies should examine the hypothesis of distinct increased

pyramidal neuron proliferation caused by LPC-DHA and MSCs *in vitro* and *in vivo* by for example flow cytometry and a bromodeoxyuridine (BrdU) assay.
The effect of an increased CTIP2+ pyramidal neuron density is still unclear. Potentially, the increased pyramidal neuron density can cause a disbalance in excitation capacity between the contralateral and ipsilateral side. An excitation-inhibition disbalance due to differences in pyramidal neuron density has already been observed after schizophrenia and similarly could result in lasting effects in functional outcome of HI injured mice (14). Future studies should confirm if pyramidal neuron density aligns with behavioural alterations in HI injured mice.

All in all, our study indicates combining LPC-DHA and MSCs is a non-invasive, promising treatment option to restore brain injury after perinatal HI. LPC-DHA and MSCs probably have distinct functions, aiding in brain recovery in a parallel manner. As optimal dosing and timing and the complete working mechanism is not fully known yet, future research should further optimize and unravel the mechanism behind a treatment with LPC-DHA and MSCs to get closer to improving the treatment for infants suffering from HI injury.

5. References

1. Gunn AJ, Thoresen M. Neonatal encephalopathy and hypoxic-ischemic encephalopathy. Handb Clin Neurol. 2019;162:217–37.
2. Yıldız EP, Ekici B, Tatlı B. Neonatal hypoxic ischemic encephalopathy: an update on disease pathogenesis and treatment. Expert Rev Neurother. 2017 May;17(5):449–59.
3. Douglas-Escobar M, Weiss MD. Hypoxic-ischemic encephalopathy: a review for the clinician. JAMA Pediatr. 2015 Apr;169(4):397–403.
4. Barnett A, Mercuri E, Rutherford M, Haataja L, Frisone MF, Henderson S, et al. Neurological and perceptual-motor outcome at 5 - 6 years of age in children with neonatal encephalopathy: relationship with neonatal brain MRI. Neuropediatrics. 2002 Oct;33(5):242–8.
5. Al-Macki N, Miller SP, Hall N, Shevell M. The spectrum of abnormal neurologic outcomes subsequent to term intrapartum asphyxia. Pediatr Neurol. 2009 Dec;41(6):399–405.
6. Papazian O. [Neonatal hypoxic-ischemic encephalopathy]. Medicina (B Aires). 2018;78 Suppl 2:36–41.
7. Koeling (hypothermie) - Het WKZ [Internet]. [cited 2023 Jun 19]. Available from: https://www.hetwkz.nl/nl/behandeling/koeling-hypothermie/folder
8. Wassink G, Davidson JO, Dhillon SK, Zhou K, Bennet L, Thoresen M, et al. Therapeutic Hypothermia in Neonatal Hypoxic-Ischemic Encephalopathy. Curr Neurol Neurosci Rep. 2019 Jan 14;19(2):2.
9. Jacobs S, Hunt R, Tarnow-Mordi W, Inder T, Davis P. Cooling for newborns with hypoxic ischaemic encephalopathy. Cochrane Database Syst Rev. 2003;(4):CD003311.
10. Shankaran S, Laptook AR, Pappas A, McDonald SA, Das A, Tyson JE, et al. Effect of depth and duration of cooling on deaths in the NICU among neonates with hypoxic ischemic encephalopathy: a randomized clinical trial. JAMA. 2014 Dec 31;312(24):2629–39.
11. Shankaran S, Laptook AR, Ehrenkranz RA, Tyson JE, McDonald SA, Donovan EF, et al. Whole-body hypothermia for neonates with hypoxic-ischemic encephalopathy. N Engl J Med. 2005 Oct 13;353(15):1574–84.
12. Suganuma H, Okumura A, Kitamura Y, Shoji H, Shimizu T. Effect of hypoxic-ischemic insults on the composition of fatty acids in the brain of neonatal rats. Ann Nutr Metab. 2013 Jan 30;62(2):123–8.
13. Brandt MJV, Nijboer CH, Nessel I, Mutshiya TR, Michael-Titus AT, Counotte DS, et al. Nutritional Supplementation Reduces Lesion Size and Neuroinflammation in a Sex-Dependent Manner in a Mouse Model of Perinatal Hypoxic-Ischemic Brain Injury. Nutrients. 2021 Dec 30;14(1).
14. Palacios-Pelaez R, Lukiw WJ, Bazan NG. Omega-3 essential fatty acids modulate initiation and progression of neurodegenerative disease. Mol Neurobiol. 2010 Jun;41(2–3):367–74.
15. Zirpoli H, Chang CL, Carpentier YA, Michael-Titus AT, Ten VS, Deckelbaum RJ. Novel Approaches for Omega-3 Fatty Acid Therapeutics: Chronic Versus Acute Administration to Protect Heart, Brain, and Spinal Cord. Annu Rev Nutr. 2020 Sep 23;40:161–87.
16. Green JT, Orr SK, Bazinet RP. The emerging role of group VI calcium-independent phospholipase A2 in releasing docosahexaenoic acid from brain phospholipids. J Lipid Res. 2008 May;49(5):939–44.
17. Martínez M, Mougan I. Fatty acid composition of human brain phospholipids during normal development. J Neurochem. 1998 Dec;71(6):2528–33.
18. Uauy R, Dangour AD. Nutrition in brain development and aging: role of essential fatty acids. Nutr Rev. 2006 May;64(5 Pt 2):S24-33; discussion S72.
19. Wagenaar N, Nijboer CH, van Bel F. Repair of neonatal brain injury: bringing stem cell-based therapy into clinical practice. Dev Med Child Neurol. 2017 Oct;59(10):997–1003.
20. Donega V, Nijboer CH, van Tilborg G, Dijkhuizen RM, Kavelaars A, Heijnen CJ. Intranasally administered mesenchymal stem cells promote a regenerative niche for repair of neonatal ischemic brain injury. Exp Neurol. 2014 Nov;261:53–64.
21. Donega V, van Velthoven CTJ, Nijboer CH, van Bel F, Kas MJH, Kavelaars A, et al. Intranasal mesenchymal stem cell treatment for neonatal brain damage: long-term cognitive and sensorimotor improvement. PLoS ONE. 2013 Jan 3;8(1):e51253.
22. Donega V, Nijboer CH, van Velthoven CTJ, Youssef SA, de Bruin A, van Bel F, et al. Assessment of long-term safety and efficacy of intranasal mesenchymal stem cell treatment for neonatal brain injury in the mouse. Pediatr Res. 2015 Nov;78(5):520–6.

23. The Clinical Trial of CL2020 Cells for Neonatal Hypoxic Ischemic Encephalopathy - Full Text View - ClinicalTrials.gov [Internet]. [cited 2023 May 18]. Available from: https://clinicaltrials.gov/ct2/show/NCT04261335?term=mesenchymal+stem+cells&cond=Hypoxic-Ischemic+Encephalopathy&draw=2&rank=4
24. A Clinical Trial to Determine the Safety and Efficacy of Hope Biosciences Autologous Mesenchymal Stem Cell Therapy for the Treatment of Traumatic Brain Injury and Hypoxic-Ischemic Encephalopathy - Full Text View - ClinicalTrials.gov [Internet]. [cited 2023 May 18]. Available from: https://clinicaltrials.gov/ct2/show/NCT04063215?term=mesenchymal+stem+cells&cond=Hypoxic-Ischemic+Encephalopathy&draw=2&rank=3
25. Neural Progenitor Cell and Paracrine Factors to Treat Hypoxic Ischemic Encephalopathy - Full Text View - ClinicalTrials.gov [Internet]. [cited 2023 May 18]. Available from: https://clinicaltrials.gov/ct2/show/NCT02854579?term=mesenchymal+stem+cells&cond=Hypoxic-Ischemic+Encephalopathy&draw=2&rank=2
26. Umbilical Cord Derived Mesenchymal Stem Cells Therapy in Hypoxic Ischemic Encephalopathy - Full Text View - ClinicalTrials.gov [Internet]. [cited 2023 May 18]. Available from: https://clinicaltrials.gov/ct2/show/NCT01962233?term=mesenchymal+stem+cells&cond=Hypoxic-Ischemic+Encephalopathy&draw=2&rank=1
27. Baak LM, Wagenaar N, van der Aa NE, Groenendaal F, Dudink J, Tataranno ML, et al. Feasibility and safety of intranasally administered mesenchymal stromal cells after perinatal arterial ischaemic stroke in the Netherlands (PASSIoN): a first-in-human, open-label intervention study. Lancet Neurol. 2022 Jun;21(6):528–36.
28. Farquharson J, Cockburn F, Patrick WA, Jamieson EC, Logan RW. Infant cerebral cortex phospholipid fatty-acid composition and diet. Lancet. 1992 Oct 3;340(8823):810–3.
29. Pu H, Guo Y, Zhang W, Huang L, Wang G, Liou AK, et al. Omega-3 polyunsaturated fatty acid supplementation improves neurologic recovery and attenuates white matter injury after experimental traumatic brain injury. J Cereb Blood Flow Metab. 2013 Sep;33(9):1474–84.
30. Paterniti I, Impellizzeri D, Di Paola R, Esposito E, Gladman S, Yip P, et al. Docosahexaenoic acid attenuates the early inflammatory response following spinal cord injury in mice: in-vivo and in-vitro studies. J Neuroinflammation. 2014 Jan 10;11:6.
31. Williams JJ, Mayurasakorn K, Vannucci SJ, Mastropietro C, Bazan NG, Ten VS, et al. N-3 fatty acid rich triglyceride emulsions are neuroprotective after cerebral hypoxic-ischemic injury in neonatal mice. PLoS ONE. 2013 Feb 20;8(2):e56233.
32. Mayurasakorn K, Niatsetskaya ZV, Sosunov SA, Williams JJ, Zirpoli H, Vlasakov I, et al. DHA but Not EPA Emulsions Preserve Neurological and Mitochondrial Function after Brain Hypoxia-Ischemia in Neonatal Mice. PLoS ONE. 2016 Aug 11;11(8):e0160870.
33. Sugasini D, Yalagala PCR, Goggin A, Tai LM, Subbaiah PV. Enrichment of brain docosahexaenoic acid (DHA) is highly dependent upon the molecular carrier of dietary DHA: lysophosphatidylcholine is more efficient than either phosphatidylcholine or triacylglycerol. J Nutr Biochem. 2019 Dec;74:108231.
34. Vannucci SJ, Back SA. The Vannucci Model of Hypoxic-Ischemic Injury in the Neonatal Rodent: 40 years Later. Dev Neurosci. 2022 Mar 9;44(4–5):186–93.
35. Guan J, Mathai S, Harris P, Wen JY, Zhang R, Brimble M, et al. Peripheral administration of a novel diketopiperazine, NNZ 2591, prevents brain injury and improves somatosensory-motor function following hypoxia-ischemia in adult rats. Neuropharmacology. 2007 Nov;53(6):749–62.
36. Inoue T, Tanaka M, Masuda S, Ohue-Kitano R, Yamakage H, Muranaka K, et al. Omega-3 polyunsaturated fatty acids suppress the inflammatory responses of lipopolysaccharide-stimulated mouse microglia by activating SIRT1 pathways. Biochim Biophys Acta Mol Cell Biol Lipids. 2017 May;1862(5):552–60.
37. DeGiosio RA, Grubisha MJ, MacDonald ML, McKinney BC, Camacho CJ, Sweet RA. More than a marker: potential pathogenic functions of MAP2. Front Mol Neurosci. 2022 Sep 16;15:974890.
38. Ye Q, Wu Y, Wu J, Zou S, Al-Zaazaai AA, Zhang H, et al. Neural Stem Cells Expressing bFGF Reduce Brain Damage and Restore Sensorimotor Function after Neonatal Hypoxia-Ischemia. Cell Physiol Biochem. 2018;45(1):108–18.

39. Anand KS, Dhikav V. Hippocampus in health and disease: An overview. Ann Indian Acad Neurol. 2012 Oct;15(4):239–46.
40. Akimov MG, Ashba AM, Fomina-Ageeva EV, Gretskaya NM, Myasoedov NF, Bezuglov VV. Neuroprotective Action of Amidic Neurolipins in Models of Neurotoxicity on the Culture of Human Neural-Like Cells SH-SY5Y. Dokl Biochem Biophys. 2019 Mar;485(1):141–4.
41. Shimazawa M, Nakajima Y, Mashima Y, Hara H. Docosahexaenoic acid (DHA) has neuroprotective effects against oxidative stress in retinal ganglion cells. Brain Res. 2009 Jan 28;1251:269–75.
42. Wang F, Bhat K, Doucette M, Zhou S, Gu Y, Law B, et al. Docosahexaenoic acid (DHA) sensitizes brain tumor cells to etoposide-induced apoptosis. Curr Mol Med. 2011 Aug;11(6):503–11.
43. Xu J, Ji T, Li G, Zhang H, Zheng Y, Li M, et al. Lactate attenuates astrocytic inflammation by inhibiting ubiquitination and degradation of NDRG2 under oxygen-glucose deprivation conditions. J Neuroinflammation. 2022 Dec 26;19(1):314.
44. Wang D-P, Kang K, Sun J, Lin Q, Lv Q-L, Hai J. URB597 and Andrographolide Improve Brain Microvascular Endothelial Cell Permeability and Apoptosis by Reducing Oxidative Stress and Inflammation Associated with Activation of Nrf2 Signaling in Oxygen-Glucose Deprivation. Oxid Med Cell Longev. 2022 May 12;2022:4139330.
45. Bhowmick S, Moore JT, Kirschner DL, Curry MC, Westbrook EG, Rasley BT, et al. Acidotoxicity via ASIC1a Mediates Cell Death during Oxygen Glucose Deprivation and Abolishes Excitotoxicity. ACS Chem Neurosci. 2017 Jun 21;8(6):1204–12.
46. Ren Z, Chen L, Wang Y, Wei X, Zeng S, Zheng Y, et al. Activation of the Omega-3 Fatty Acid Receptor GPR120 Protects against Focal Cerebral Ischemic Injury by Preventing Inflammation and Apoptosis in Mice. J Immunol. 2019 Feb 1;202(3):747–59.
47. Plemel JR, Michaels NJ, Weishaupt N, Caprariello AV, Keough MB, Rogers JA, et al. Mechanisms of lysophosphatidylcholine-induced demyelination: A primary lipid disrupting myelinopathy. Glia. 2018 Feb;66(2):327–47.
48. Ahmmed MK, Hachem M, Ahmmed F, Rashidinejad A, Oz F, Bekhit AA, et al. Marine Fish-Derived Lysophosphatidylcholine: Properties, Extraction, Quantification, and Brain Health Application. Molecules. 2023 Mar 30;28(7).
49. Belayev L, Marcheselli VL, Khoutorova L, Rodriguez de Turco EB, Busto R, Ginsberg MD, et al. Docosahexaenoic acid complexed to albumin elicits high-grade ischemic neuroprotection. Stroke. 2005 Jan;36(1):118–23.
50. Kulkarni PG, Balasubramanian N, Manjrekar R, Banerjee T, Sakharkar A. DNA Methylation-Mediated Mfn2 Gene Regulation in the Brain: A Role in Brain Trauma-Induced Mitochondrial Dysfunction and Memory Deficits. Cell Mol Neurobiol. 2023 May 16;
51. Barker R, Wellington D, Esiri MM, Love S. Assessing white matter ischemic damage in dementia patients by measurement of myelin proteins. J Cereb Blood Flow Metab. 2013 Jul;33(7):1050–7.
52. Kida H, Nomura S, Shinoyama M, Ideguchi M, Owada Y, Suzuki M. The effect of hypothermia therapy on cortical laminar disruption following ischemic injury in neonatal mice. PLoS ONE. 2013 Jul 23;8(7):e68877.
53. Follett PL, Rosenberg PA, Volpe JJ, Jensen FE. NBQX attenuates excitotoxic injury in developing white matter. J Neurosci. 2000 Dec 15;20(24):9235–41.
54. Shao R, Sun D, Hu Y, Cui D. White matter injury in the neonatal hypoxic-ischemic brain and potential therapies targeting microglia. J Neurosci Res. 2021 Apr;99(4):991–1008.
55. Shinoyama M, Ideguchi M, Kida H, Kajiwara K, Kagawa Y, Maeda Y, et al. Cortical region-specific engraftment of embryonic stem cell-derived neural progenitor cells restores axonal sprouting to a subcortical target and achieves motor functional recovery in a mouse model of neonatal hypoxic-ischemic brain injury. Front Cell Neurosci. 2013 Aug 21;7:128.
56. Angevine JB, Sidman RL. Autoradiographic study of cell migration during histogenesis of cerebral cortex in the mouse. Nature. 1961 Nov 25;192:766–8.
57. Larsen DD, Callaway EM. Development of layer-specific axonal arborizations in mouse primary somatosensory cortex. J Comp Neurol. 2006 Jan 20;494(3):398–414.
58. Keilhoff G, John R, Langnaese K, Schweizer H, Ebmeyer U. Triggered by asphyxia neurogenesis seems not to be an endogenous repair mechanism, gliogenesis more like it. Neuroscience. 2010 Dec 15;171(3):869–84.

59. Nakatomi H, Kuriu T, Okabe S, Yamamoto S, Hatano O, Kawahara N, et al. Regeneration of hippocampal pyramidal neurons after ischemic brain injury by recruitment of endogenous neural progenitors. Cell. 2002 Aug 23;110(4):429–41.
60. Donega V, Nijboer CH, Braccioli L, Slaper-Cortenbach I, Kavelaars A, van Bel F, et al. Intranasal administration of human MSC for ischemic brain injury in the mouse: in vitro and in vivo neuroregenerative functions. PLoS ONE. 2014 Nov 14;9(11):e112339.

6. Supplementary

6.1 A hit with 60 µM H_2O_2 creates a rescue window for the *in vitro* examination of oxidative stress

In order to create an H_2O_2 hit model to examine the effect of DHA and LPC-DHA, a separate dose response curve was composed for H_2O_2 with and without DMSO. At 60 µM H_2O_2, a significant reduction in cell viability was found in both hit models ($p<0.0001$, $p<0.0001$, Fig S1). Therefore, this concentration was chosen in the H_2O_2 hit model for further experiments combined with DHA and LPC-DHA.

6.2 A hit with 2800 nM etoposide creates a rescue window for the *in vitro* examination of DNA damage

Likewise the H_2O_2 hit model, a separate dose response curve was composed for etoposide with and without DMSO. At 2800 nM etoposide, a significant reduction in cell viability was found in both hit models ($p<0.0001$, $p<0.0001$, Fig S2). Accordingly, 2800 nM etoposide was used in the *in vitro* DNA damage model and used in further experiments combined with DHA and LPC-DHA.

6.3 A 24 hour deprivation of glucose and limitation to 1% O_2 creates a rescue window for the *in vitro* OGD model

Likewise the H_2O_2 and etoposide hit model, a separate dose response curve was composed for the OGD model with and without DMSO. To find the optimal rescue window, different OGD exposure and reperfusion times were studied. A significant hit effect has been found after an OGD exposure of 24 hours without reperfusion in both models ($p<0.0001$, $p<0.0001$, Supplementary Fig S3). Accordingly, OGD24R0 was used in the *in vitro* OGD model and used for further experiments combined with DHA and LPC-DHA.

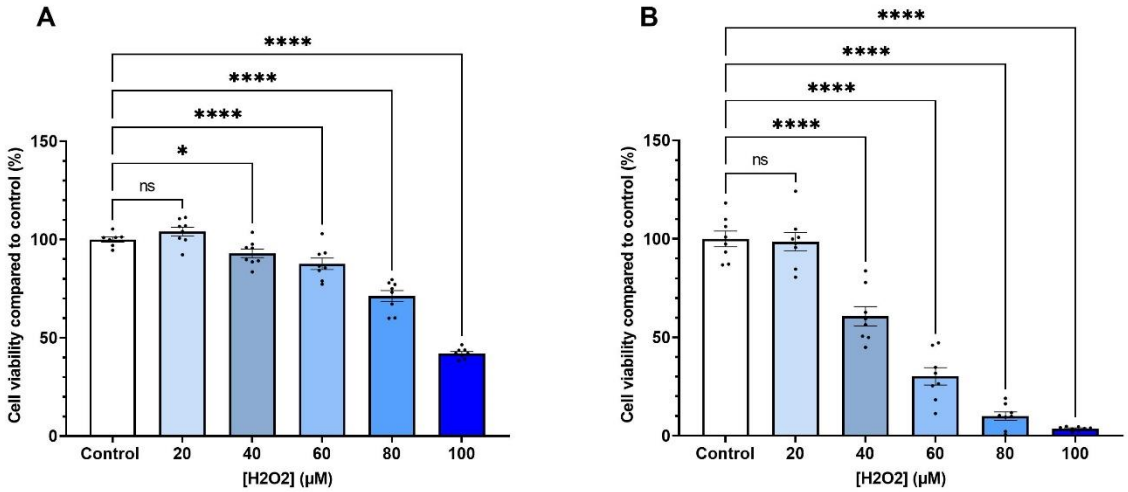

Fig S1. H_2O_2 dose response curves. A) H_2O_2 dose response curve in medium. 0 µM, n=7; 20 µM, n=8; 40 µM, n=8; 60 µM, n=8; 80 µM, n=8; 100 µM, n=8. B) H_2O_2 dose response curve in medium with 0.0175% DMSO. Control, n=8; 20 µM, n=8; 40 µM, n=8; 60 µM, n=8; 80 µM, n=8; 100 µM, n=8. * $p<0.05$. **** $p<0.0001$. Data represents mean + SEM.

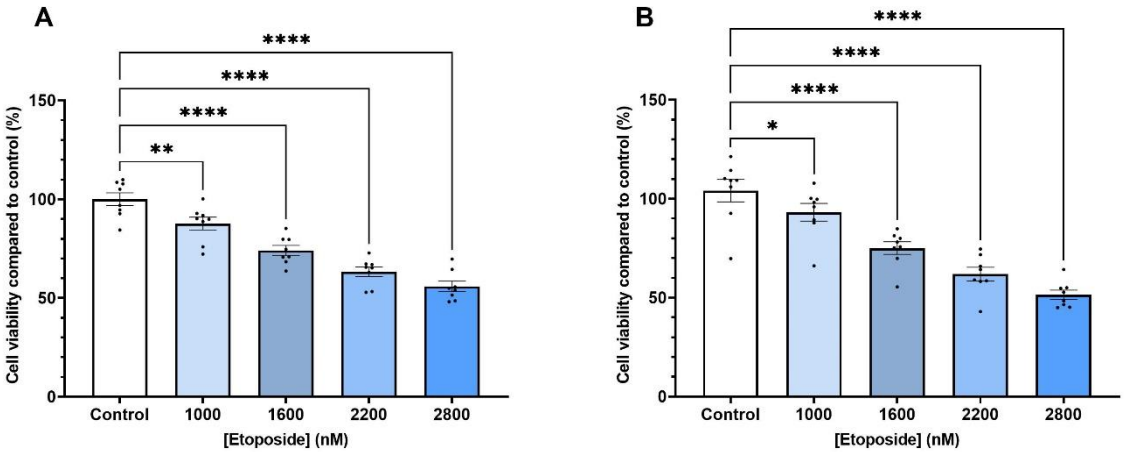

Fig S2. Etoposide dose response curves. A) Etoposide dose response curve in medium. Control, n=8; 1000 nM, n=8; 1600 nM, n=8; 2200 nM, n=8; 2800 nM, n=8. B) Etoposide dose response curve in medium with 0.0175% DMSO. Control, n=8; 1000 nM, n=8; 1600 nM, n=8; 2200 nM, n=8; 2800 nM, n=8. * p<0.05. ** p<0.01. *** p<0.001 **** p<0.0001. Data represents mean + SEM.

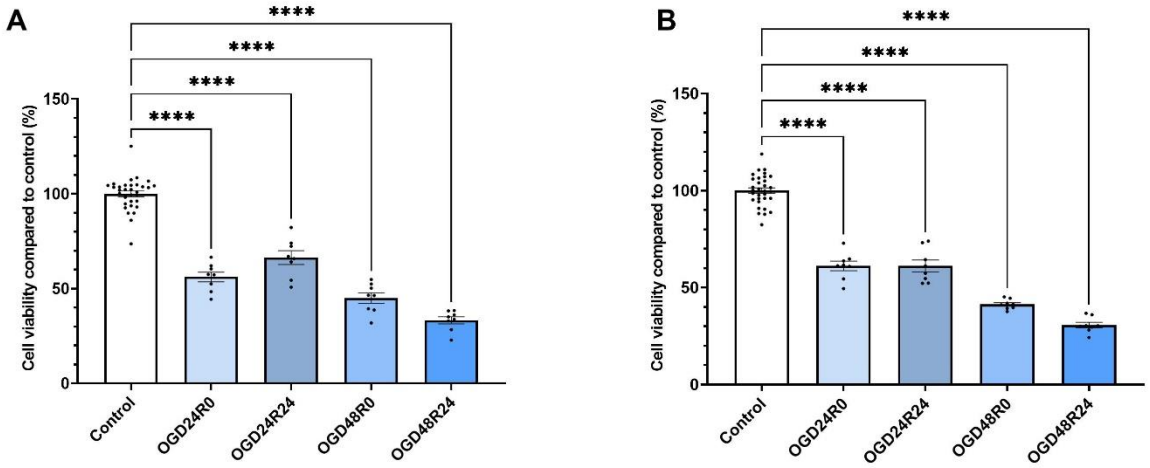

Fig S3. Relative cell viability after deprivation of glucose and limitation to 1% O_2. A) OGD hit effect in medium with 0.025% BSA. Control, n= 32; OGD24R0, n=8; OGD24R24, n=8; OGD48R0, n=8; OGD48R24, n=8. B) OGD hit effect in medium with 0.0175% DMSO. Control, n= 32; OGD24R0, n=8; OGD24R24, n=8; OGD48R0, n=8; OGD48R24, n=8 OGD = oxygen glucose deprivation; R = reperfusion. **** p<0.0001. Data represents mean + SEM.